

Scattered Light from the Earth Limb Measured with the STIS CCD

Dick Shaw, Merle Reinhart, and Jennifer Wilson

17 June 1998

ABSTRACT

We describe a recent program to measure the amount of scattered light near the Earth limb with the STIS CCD detector. Scattered Earth light is only marginally detected as close as 11° from the dark limb, but it is easily detected within 25° from the bright limb, and it can vary in brightness by nearly a factor of two on timescales as short as two minutes. The measured background level is essentially constant between 25° and 37° from the bright Earth limb, but it increases exponentially and uniformly over the entire detector within 25° of the bright limb; within 20° the light distribution on the images becomes spatially non-uniform at a level exceeding $1-\sigma$ deviations from the read noise.

1. Introduction

The background in UV and optical images obtained with *HST* comes from three primary sources: Earth shine, geocoronal emission, and zodiacal light. The angular and temporal dependencies of the latter two sources have been successfully modeled, and are described for STIS in the *STIS Instrument Handbook* (Walborn & Baum 1998). It is more difficult, however, to predict the effect that Earth shine will have on STIS science programs without direct measurement. The effect on imaging programs is important to understand, particularly when observing targets in the continuous viewing zone (CVZ), which is centered on the *HST* orbit pole.

We present here the results of the Cycle 7 calibration program 7646, whose purpose was to quantify the amount and character of scattered light near the Earth limb at optical wavelengths. The observational program is described in §2, and the analysis and a comparison with a detailed background model is presented in §3. We conclude in §4 with recommendations for limb-angle constraints for STIS, and offer advice to observers who wish to observe targets under conditions of high background from Earth scattered light.

2. Observing Program

Alignment Strategy

Program 7646 was designed to quantify the amount of optical scattered light as a function of Earth limb angle, and to probe extreme limb angles in order to set a firm limit for imaging science programs. Since our goal was to orient *HST* to sample particular limb angles and avoid diffuse astronomical targets, rather than to observe particular astronomical targets in spite of limb angle constraints, our approach to the design of the observing program was necessarily somewhat unusual. It was essential that the change of limb angle with time be kept small, at least when the limb angle was at an extremum. We therefore chose orientations near the *HST* orbit pole. The *HST* orbit plane is inclined $28^\circ.5$ from the equator, and precesses with a period of about 56 days. When *HST* is aligned along its orbit pole (which defines the center of the CVZ) the corresponding declination is $61^\circ.5$ and the Earth limb angle is approximately 24° . For ease in specifying the observing program, we constrained the scheduling window such that a change in limb angle could be effected solely by changing the declination of the target coordinates. This condition is satisfied when the *HST* orbital pole is oriented toward or away from the sun.

Since our strategy for measuring the scattered light was to measure the background level on a sequence of images, we chose the *HST* alignments with some care to avoid extended celestial targets, such as nebulae, the stellar background of the Galactic plane, and the Magellanic Clouds. We also avoided stars bright enough to saturate the CCD to minimize the effect of charge bleeding along columns. A log of the observations is given in Table 1.

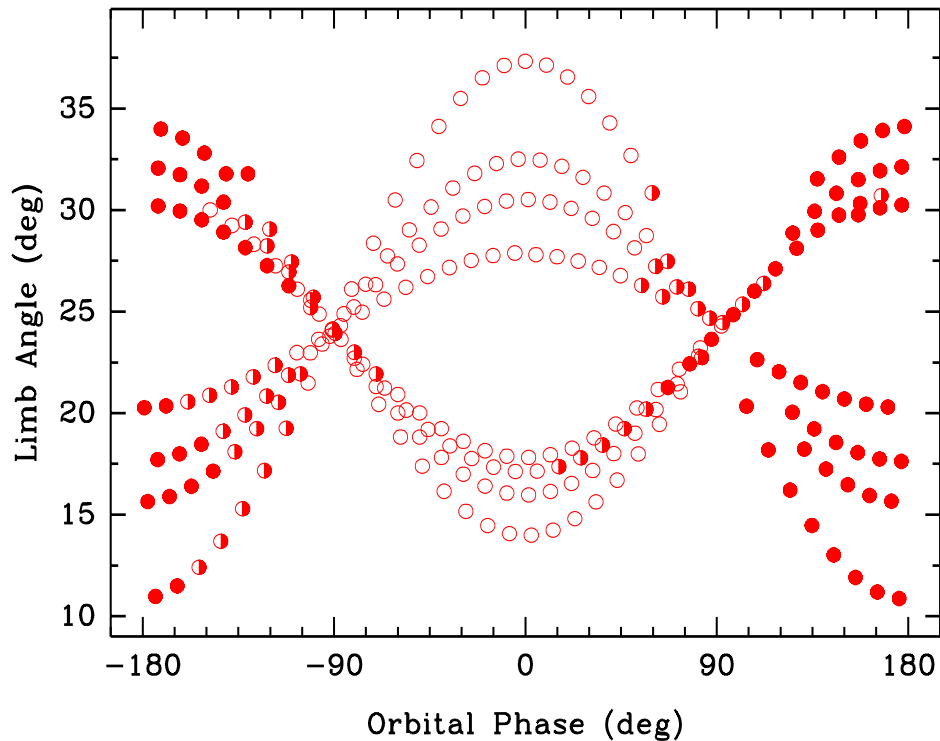
Table 1: Log of Observations for Program 7646

Target	U.T. Date	R.A. (deg)	Declination (deg)	Bright Earth Limb Angle (deg)	Dark Earth Limb Angle (deg)
CVZ-SUN-1	10-Dec-97	257.680	71.530	14.0	34.0
CVZ-SUN-2	10-Dec-97	257.450	69.515	16.0	32.0
CVZ-SUN-3	11-Dec-97	257.440	67.440	18.1	29.9
CVZ-SUN-4	9-Dec-97	257.670	64.510	17.1	30.9
CVZ-SUN-5	11-Dec-97	257.430	58.450	27.0	21.0
CVZ-SUN-6	12-Dec-97	257.578	55.539	30.0	18.0
CVZ-SUN-7	12-Dec-97	257.680	53.520	32.0	16.0
CVZ-SUN-8	13-Dec-97	257.000	51.505	37.3	10.9

The Exposures

We used the CCD detector with the clear (50CCD) aperture and GAIN=1 for greatest sensitivity, and because this aperture/gain combination is a likely choice for deep imaging projects. We planned a set of four contiguous, CR-SPLIT=8 exposures of 16 min duration each¹ which, including exposure overhead and buffer dumps, filled up a full 96-min orbit for each visit. The 2 min integrations were short enough to avoid sampling a large range in limb angle (always $<1^\circ.2$ even near the Earth terminator), but were still sufficient to detect scattered light at a low level. All exposures were obtained with gyro-mode guiding. Figure 1 shows the limb angle coverage for the exposures in this program. The orbital phase is the position of *HST* in its orbit, adjusted so that zero corresponds to the extremum of the bright limb angle for each visit. Note that zero phase does not necessarily correspond to the mid-point of the bright Earth limb passage. The reason is that the observations could not all be scheduled on the day when the *HST* orbit pole was aligned toward the sun. The effect of changing the date by a few days from optimum (but leaving the R.A. of the target unchanged) is to shift the mid-point of the bright Earth limb passage relative to orbital phase zero. This has no effect on the following analysis.

Figure 1: Limb angle coverage for the exposures in program 7646. Exposures taken near orbital phase zero were obtained near the bright Earth limb (*open circles*), exposures near phase $\pm 90^\circ$ were obtained near twilight (*half-filled circles*), and exposures near $\pm 180^\circ$ were obtained near the dark Earth limb (*filled circles*).



1. The last of the four exposures was 15^m20^s in duration to allow for the visit-level overhead.

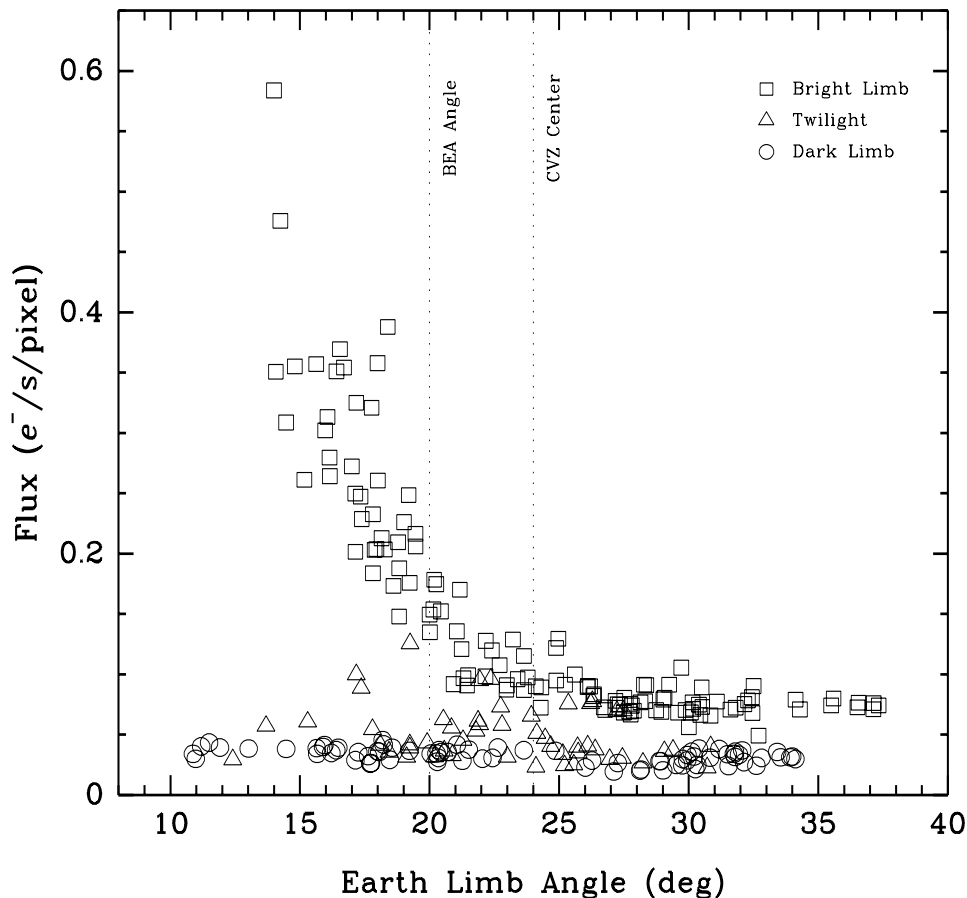
3. Measurement of the Background

Inspection of the image histograms showed that the image mode was the best indicator of the background sky level. The limb angles associated with each exposure were derived from the definitive orbital ephemeris for *HST* during the time of the observations.

Variation with Limb Angle

The variation of image background with Earth limb angle is plotted in Fig. 2. The angle in this plot is the separation from the nearest Earth limb, be it dark or bright; different symbols in the plot denote bright limb, dark limb, or twilight. Several features are evident. The background near the dark Earth limb is nearly constant at all sampled separations, with a value near 0.033 electrons/s/pixel. The background for bright Earth limb angles larger than 25° is also fairly constant, at ~ 0.075 electrons/s/pixel. We attribute background levels observed in Earth shadow to the effect of zodiacal light, and background levels higher than that to scattered Earth light. The constancy of the background at large limb angles on the bright side of the Earth is somewhat puzzling: we would have expected the background to continue to decline with increasing angle from the bright limb, and approach that observed in Earth shadow as the limb angle approached the “LOW-SKY” limit of 40° . This question deserves further investigation, probably with the support of a detailed background model for *HST*.

Figure 2: The measured background flux is a strong function of angle for exposures within 25° of the bright Earth limb (*open squares*), but it is nearly independent of angle for exposures near the dark limb (*open circles*). Exposures obtained while passing the Earth terminator are marked as twilight (*open triangles*). The limb angles corresponding to the CVZ center and the current bright Earth avoidance angle are marked (*dotted lines*) for reference.



Perhaps the most striking of Fig. 2 is the dramatic rise in the background for Earth limb angles less than about 25°. Figure 3 shows that the increase in background level with decreasing limb angle is well characterized by an exponential; a power law fit gives:

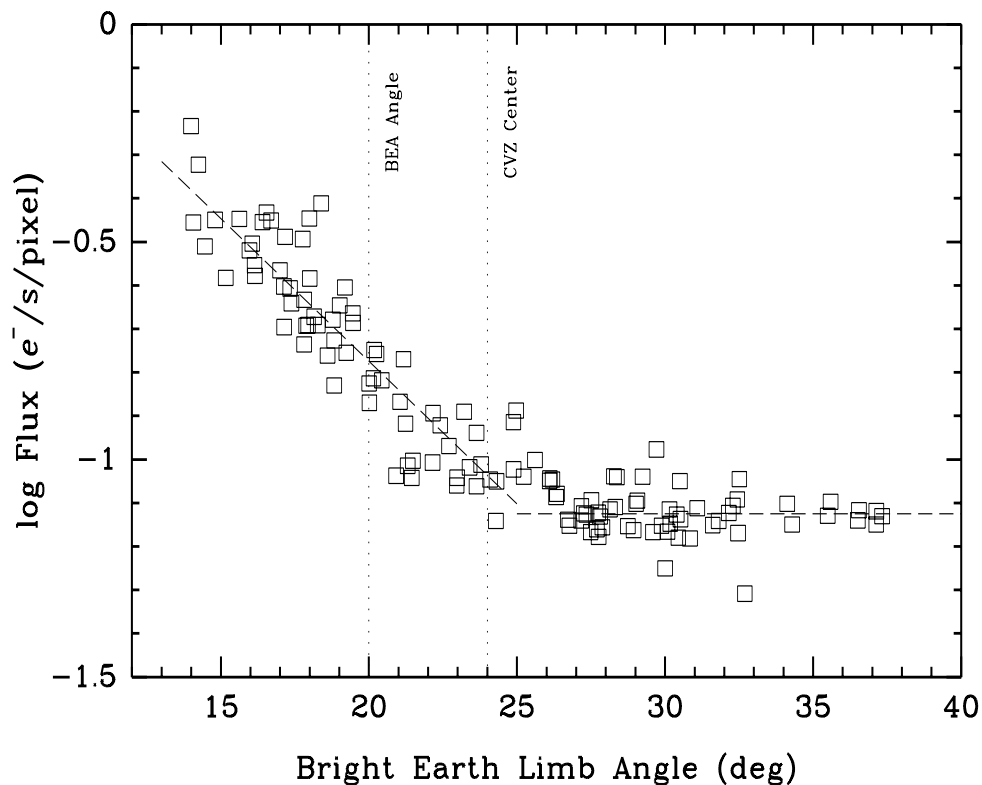
$$C_{BG} = 3.4564 \times 10^{-0.06564\alpha}$$

where the background count rate C_{BG} is in electrons/s/pixel,

and the limb angle, α , is in degrees. A rough² conversion to surface flux (in ergs/s/cm²/arcsec²) requires a multiplication by PHOTFLAM (8.968 x 10⁻²⁰ erg/s/cm²/count) and dividing by the square of the plate scale (0.0508 arcsec/pixel). Regrettably, the onset of the rise occurs for limb angles such as those encountered near the CVZ, which will complicate the data analysis for certain science programs (see §4 below).

2. Note that the PHOTFLAM value is derived in the calibration pipeline assuming a flat continuum for the source; a solar-type spectral energy distribution would yield a more accurate value, given the extremely broad effective bandpass of the clear aperture.

Figure 3: The measured background flux near the bright Earth limb, showing the constant background for angles greater than $\sim 25^\circ$, and the exponential rise for smaller angles (*dashed lines*). The limb angles corresponding to the CVZ center and the current bright Earth avoidance angle are marked (*dotted lines*) for reference.



Field-Dependent Variations

For most images, the background is spatially uniform. However, substantial gradients become apparent for limb angles less than 15° . The background for the image obtained at the most extreme bright limb angle is strongest at low x - and high y -coordinates, as shown in Fig. 4. Images taken just before and just after this image (but at the same limb angle) show a much lower dependence on x , but roughly the same dependence on y . The orientation of the brightness gradient in Fig. 4 is along the spacecraft $-V3$ axis, which was oriented toward the bright Earth at the time of the exposure. We suppose that this extreme field dependence results from light scattering off a baffle or some other component of the OTA and directly into the STIS aperture. The field-dependent variations can even be important for limb angles near 20° , as is shown in Fig. 5. The brightness variation across this image is comparable to a $1\text{-}\sigma$ deviation from the CCD read noise.

Figure 4: Image from visit 1, exposure 3, CR-SPLIT 7, showing the variation in background level from near 50 electrons (*lower right*) to nearly 300 electrons (*upper left*).

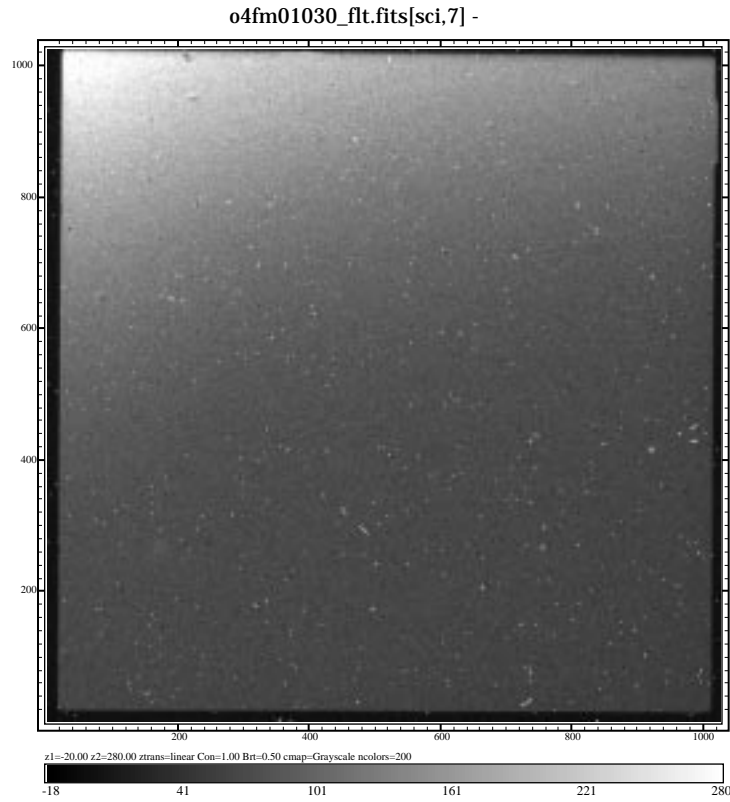
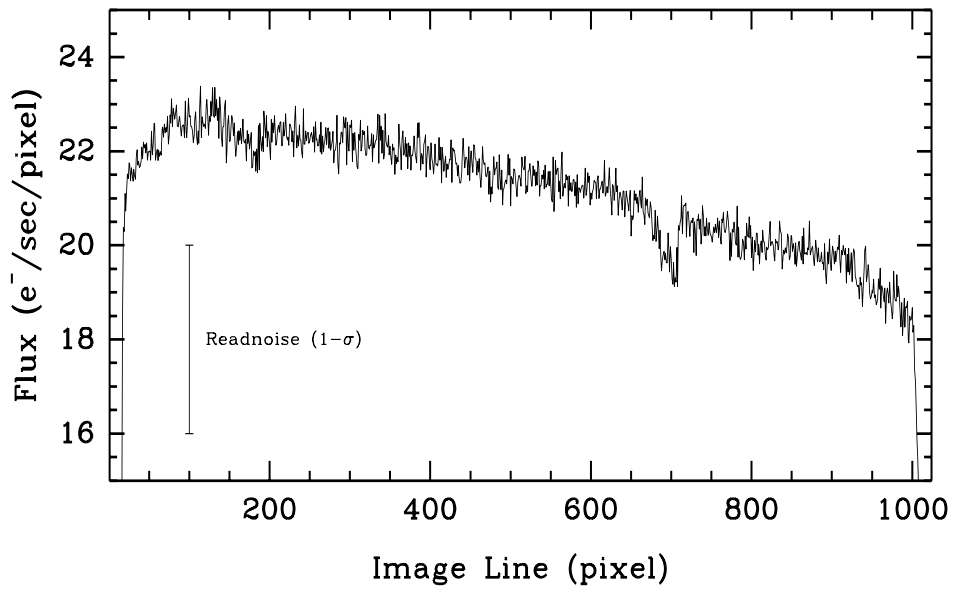


Figure 5: The background field dependence for an image obtained at $19^\circ.2$ from the bright Earth limb. The magnitude ($1-\sigma$) of the CCD read noise is shown for comparison.

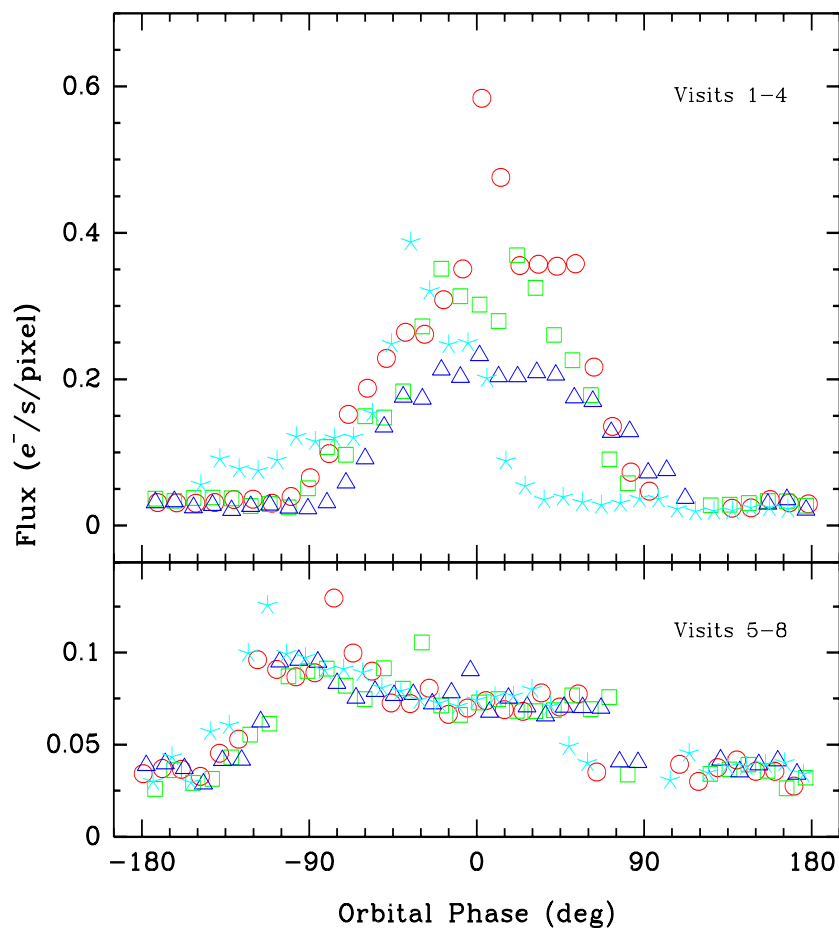


Temporal and Azimuthal Variations

Both Figs. 1 and 2 show that the range of background levels encountered for a nearly constant limb angle can vary by several tens of percent, which is much larger than the measurement error. This variation can occur on timescales as short as three minutes, as shown in Fig. 6. That both the brightness and field-dependence of the background can vary on such short timescales suggests that the cause is the varying reflectivity of the terrain over which *HST* passes during the course of an orbit. That is, whether the illuminated Earthscape as seen from *HST* is dominated by land mass, ocean, or clouds could account for the short-term variation the image background level.

We also examined the azimuthal dependence of the background level—i.e., for a small range of limb angles, does the background level depend upon the deviation of the V3 axis from the plane defined by the sun-Earth-*HST*? We found no correlation, or at least none that exceeded the $\sim 50\%$ temporal background variations.

Figure 6: Variation in sky background with orbital phase, where different symbols are used for each visit. The difference in orbital phase of $\sim 10^\circ$ between successive exposures corresponds to the $\sim 2^m45^s$ elapsed time from the start of one exposure to the next in a CR-SPLIT series.



Comparison with an HST Background Model

A rough parameterization of the existing background model for HST is used in the STIS exposure time calculators (ETCs), which are used extensively by the GO/GTO community for planning observations. It is therefore important to explore the extent to which the background level computed by the ETCs is consistent with the results presented here. A comparison of the observed background and that predicted from the ETC (for the same aperture and exposure time) is presented in Table 2. We used an “average” zodiacal light

Table 2: Comparison of ETC with Observed Background

Earthshine Parameter	ETC Prediction (counts/s/pixel)	Obs. Earth Limb Angle
Shadow	0.033	Any (shadow)
Average	0.112	22°.7
High	0.193	19°.1

contribution, since the agreement between the ETC and the observations in Earth shadow was perfect. The predicted count rate is listed in column 2 for each of the three available settings of the “Earth-shine” ETC parameter. We list in column 3 the bright Earth limb angle at which this flux was observed, based upon the relations given at the beginning of this section. We note that the ETC prediction for the “average” Earth shine is typical of a background found quite close to the bright Earth avoidance angle; the prediction for “high” Earth shine would require observing at or within the BEA. Such conditions would actually be quite rare unless the observations were obtained near the CVZ. We conclude that the model of the Earth shine used in the current STIS ETCs leads to over-predictions of the background by several tens of percent, which will be corrected in the near future.

4. Discussion and Recommendations

The background level in STIS CCD images can be substantial if they are obtained near the bright Earth limb, particularly at low gain settings. Fortunately, most actual exposures will scarcely be affected by scattered Earth light, since low limb angles are usually encountered only for brief periods near the end of the target visibility period. But for CVZ or near-CVZ targets, the effect on broad-band images will be substantial. It becomes rapidly more difficult to detect faint or low-surface brightness targets in images obtained closer than 25° from the bright Earth limb. Fortunately, for brighter targets it is straightforward to correct for this effect in the pipeline cosmic-ray rejection and in downstream analysis, even in the presence of temporal variations, as long as the background is spatially uniform. Indeed, the pipeline cosmic-ray rejection has been shown to perform well under these circumstances. However, for angles less than 20° from the bright Earth limb, the

rapid onset of field-dependent variations in the background would make calibration and analysis very challenging.

The magnitude of scattered Earth light will be very much less for the other, more commonly used STIS observing modes. For all except slit-less spectroscopic modes, the background per wavelength bin will be lower by a factor of at least a few hundred. Even in imaging mode, the effect of scattered light will be very much lower for the narrow-band and neutral density filters. The change in background with limb angle in Fig. 3 shows that exposures could be obtained very much closer to the bright Earth for these modes, without compromising the science programs.

Recommendations

At present, the operational bright Earth avoidance (BEA) angle for STIS is 20° , the same as for WFPC-2. Based on the analysis presented here, we conclude that a mode-dependent implementation of the BEA angle would be beneficial for many science programs on all instruments. For STIS, the implementation would be as follows:

- The BEA angle for broad-band imaging (including target ACQs) and slit-less spectroscopic modes should remain at 20° .
- The BEA angle for imaging with narrow-band or neutral-density filters, and for all except slit-less spectroscopic modes, be may changed to $15^\circ.5$; this is the same BEA as that for the Fine Guidance Sensors.
- The minimum BEA angle for LOW-SKY observations should remain at 40° .

Adopting (or retaining) these limits will have a few major effects. First, for spectroscopic and narrow-band imaging observations, it will open up scheduling opportunities, in that exposures can be obtained $\sim 4^\circ.5$ closer to the bright Earth limb. The increased scheduling window can be substantial for high declination targets, especially for spectroscopic observations with tight constraints on the slit orientation. Specifically, the absolute value of the declination range covered in the CVZ increases from $\sim 50^\circ\text{--}77^\circ$ to $46^\circ\text{--}77^\circ$, which would significantly increase the size of the CVZ. At the central declination of 61.5 , the region of sky within the CVZ at some time during the year would increase by at least 50%. Taken together, moving the BEA angle from 20° to $15^\circ.5$ means more targets would have CVZ opportunities, and the duration of a given CVZ opportunity will grow substantially. Enabling this mode-dependent capability will require certain upgrades to the ground system software. We recommend that a feasibility study be initiated to support a cost/benefit analysis of the proposed enhancements.

The effect of leaving the BEA angle at 20° for broad-band imaging and slit-less spectroscopy is that such observations will suffer somewhat elevated background levels if the bright Earth limb angle falls below 25° during the exposure; the magnitude of the effect will be a function of latitude above the *HST* orbit plane, which affects the duration of the shallow limb angle passage. Except for CVZ and near-CVZ targets, this effect is only

likely to apply during a brief period at the end of the target visibility. This effect extends to target ACQ exposures that may occur within 25° of the bright limb. In this case, the background could vary by $\sim 50\%$ between the paired ACQ exposures. Since the on-board processing of these images includes registering them and taking the minimum (to reject hot pixels and cosmic rays), the effect will manifest itself as an inability to reject low-level cosmic rays. The difference in the background of the paired ACQ images if obtained at the current BEA angle of 20° reaches the $3\text{-}\sigma$ level³ in ~ 140 s. Note, however, that most ACQs (unless they are for targets near the CVZ) will occur between 30° and 35° from the bright limb because they are preceded by the PCS acquisition.

The very low scattered light background near the dark Earth limb suggests that the STIS CCD can operate very well in the Earth shadow at limb angles at least as close as 11° . The current avoidance angle for the dark Earth limb is $7^\circ.6$, and we can recommend no change. Though there are scheduling and other constraints that limit the amount of Earth shadow time available for science programs, the scattered light level will not compromise the quality of STIS programs that require this resource.

Finally, we recommend a study into the feasibility, and of the cost and scientific benefit, of enhancing the scheduling system to support numeric GO constraints on background level. The good agreement between the model predictions of zodiacal light and scattered Earth light means that it should be straightforward to compute intervals when the total background level is likely to lie below a specified threshold. Such an approach would give GOs a much more direct and meaningful constraint on the desired background level than the current “LOW-SKY” and “SHADOW” special requirements.

References

Walborn, N. & S. Baum, eds. *Space Telescope Imaging Spectrograph Instrument Handbook, Version 2.0* (Baltimore: ST ScI) 1998

3. Note that if the BEA angle is reduced, the required margins for the FGS acquisitions would put the effective avoidance limit for acquisitions at $17^\circ.5$. The difference in background levels in the ACQ images would reach $3\text{-}\sigma$ in ~ 100 s in this case.